

Thermoplasmonic Membrane Distillation

Antonio Politano^{a,b}, Gianluca Di Profio^c, Vanna Sanna^d, Efrem Curcio^{e*}

^a Department of Physics, University of Calabria - Via P. Bucci Cubo 31/C, 87036 Rende (CS) Italy

^b Italian Institute of Technology, Graphene Labs, Via Morego 10, 16163 Genova, Italy

^c Institute on Membrane Technology, National Research Council of Italy ITM-CNR, Italy - Via P. Bucci Cubo 17C, 87036 Rende (CS) Italy

^d Nanomater S.r.l., Porto Conte Ricerche, Loc. Tamariglio, 07041 Alghero (SS).

^e Department of Environmental and Chemical Engineering DIATIC, University of Calabria - Via P. Bucci Cubo 45A, 87036 Rende (CS) Italy

e.curcio@unical.it

Membrane Distillation (MD) is a hybrid thermal/membrane technology emerging either as a promising alternative or as a complement to Reverse Osmosis, having the potential to concentrate saline solutions even up to supersaturation. Presently, performance of conventional MD systems is drastically affected by temperature polarization, a phenomenon intrinsically connected to the removal of latent heat due to evaporation, which causes the decrease of feed temperature at the membrane surface with respect to the bulk. As a consequence, the net driving force to mass transfer falls down along with the thermal efficiency of the process. Due to these adverse effects, technological applications of MD are still elusive. In this work, we prove that thermoplasmonic effect induced by photothermal excitations of silver nanoparticles (Ag NPs), incorporated into polyvinylidene (PVDF) membranes, remarkably increase the feed temperature at the membrane surface exposed to light radiation, thus achieving unmatched performance in a vacuum MD unit.

1. Introduction

With a global capacity currently around 100 million m³/day, the desalination market (expected to jump to \$ 50 billion by 2020) is largely dominated by membrane technology; large Seawater Reverse Osmosis (SWRO) installations exhibit an energy consumption of 3-4 kWh per m³ drinking water and a unit water cost approaching 0.5 \$/m³. However, SWRO technology still faces crucial technological challenges, mostly related to a relatively low overall recovery factor, about 30-50%, limited by concentration polarization phenomena. As a consequence, half cubic meter of brine at molar concentration of about 1 M in NaCl is produced per cubic meter of feed seawater and released in the environment. Literature studies demonstrate adverse ecological and toxicological impacts of hypersaline brines on echinoids and ascidians, sediment infauna, seagrass and epifauna, planktons, fishes and clams (Lattemann and Höpner, 2008).

MD is a hybrid thermal/membrane technology, not limited by concentration polarization, having the potential to produce desalted water at recovery factors greater than 85%. In MD, a microporous hydrophobic membrane is in contact with a heated feed solution: the hydrophobic character of the membrane prevents the permeation of molecules in liquid phase (no filtration), while sustaining a vapour-liquid interface at the pores mouth. Here, water evaporates (whereas non-volatile solutes are retained), diffuses across the membrane, and condenses on the opposite side ("distillate"). Theoretically, MD guarantees a complete rejection of non-volatile solutes such as macromolecules, colloidal species, ions etc. Relatively low temperature gradients are generally sufficient to establish a satisfactory transmembrane flux (1-10 l/m²h); typical feed temperatures vary in the range of 50-80°C, allowing the efficient recycle of low-grade or waste heat streams, as well as the use of alternative energy sources such as solar, wind or geothermal (Al-Obaidani et al., 2008; Curcio et al., 2005; Majidi Salehi et al., 2016).

The ability of MD to concentrate an aqueous solution up to supersaturation has been also exploited for the crystallization of biomolecules and active pharmaceutical ingredients (Curcio et al., 2016, Di Profio et al., 2007, Di Profio et al., 2010). Tufa et al. (2015) proposed a hybrid MD/ Reverse Electrodialysis system for

simultaneous production of water and energy from SWRO brines, thus implementing the concept of low energy and near-zero liquid discharge in seawater desalination.

Since the last decade, MD reached the demonstration stage. However, the development of advanced membrane materials able to enhance its energy efficiency is considered as a necessary step before the technological implementation at large industrial scale. Specifically, when operating with conventional microporous hydrophobic membranes, the temperature at the feed interface decreases as a consequence of the latent heat flow associated to the evaporation of volatile molecules (generally water). This adverse phenomenon, known as “temperature polarization”, significantly reduces the net driving force to the mass transport and, ultimately, drastically decreases the overall efficiency of MD.

Recently, incorporation of metal nanoparticles (NPs) into polymeric films (mixed matrix membranes) has emerged as an efficient way to apply the concept of localized plasmonic heating to membrane separation (Politano *et al.*, 2016). Thermoplasmonics, i.e. the thermal heating associated with optically resonant plasmonic excitations in metal NPs, is based on the control of nanoscale thermal hotspots by light irradiation (Baffou *et al.*, 2013). Plasmonic NPs, acting as ideal confined nanosources of heat within polymeric membranes, allow converting absorbed light radiation into heat, thus increasing the temperature of the medium surrounding the membrane interface and potentially overcoming limitations related to thermal polarization.

The heat generation rate depends on the morphology (temperature increase is proportional to the second power of the NP radius) and physical properties of the metal; Ag NPs, under plasmon resonance conditions, generate heat about ten times stronger than Au NPs (Lee *et al.*, 2004).

In this work, we investigate the thermoplasmonic heating effect promoted by Ag NPs incorporated into microporous polyvinylidene (PVDF) membranes with the aim to design an innovative photo-thermally induced MD unit. The impact of localized heating on transmembrane flux and temperature profiles for a 0.5 M NaCl solution, conventionally mimicking seawater salinity, is reported and discussed.

2. Materials and Methods

Ag nanoparticles (Ag NPs) were synthesized by the chemical reduction method with sodium citrate as metal precursor; in a typical experiment, 100 mL of 1 mM AgNO₃ aqueous solution was heated to boiling point and 10 mL of trisodium citrate aqueous solution (1 wt %) was injected.

Microporous membranes in flat-sheet configuration containing Ag NPs were prepared by nonsolvent-induced phase inversion: PVDF homopolymer powder Solef®6010 (Solvay, Italy) was mixed at room temperature with a mixture of Ag NPs in dimethylformamide (DMF) in appropriate amount to modulate Ag NPs content, and then cast on a glass plate by automated casting machine (Elcometer) using knife with gap of 150 μm, and then immersed in a water bath at 20°C. After washing with ethanol in order to remove residual traces of solvent or additives, membranes were dried in oven at 60 °C under vacuum for 24 h.

UV-VIS spectra of Ag NPs dispersed in DMF (30% w/w) with dilution factor of 200 indicated a maximum absorbance intensity around 410 nm, not far from the plasmon resonance wavelength of Ag NPs in water (Hutter *et al.*, 2001). The maximum absorbance wavelength was not significantly affected by the polymer surrounding, with a shift from 420 to 430 nm detected when increasing NPs content from 15 to 25%w/w, respectively.

SEM analysis (Quanta 200 F FEI Philips) of cross-section of the hand-made (Figure 1.a-d) indicated that membranes have a asymmetric structure, with macrovoids generally extended over 40% c.a of the membrane thickness. Morphological and physico-chemical properties of prepared membranes are reported in Table 1.

Table 1: Main properties of investigated membranes

Membrane code	Contact angle (°)	Thickness (μm)	Porosity (%)	Pore size (μm)
Unloaded PVDF-REF	86.3±2.5°	64±11	27	0.45±0.05
PVDF-15% Ag NPs	83.6±3.9°	72±14	32	0.22±0.03
PVDF-20% Ag NPs	81.4±0.74°	65±12	36	0.38±0.04
PVDF-25% Ag NPs	80.3±3.6°	60±15	22	0.40±0.05

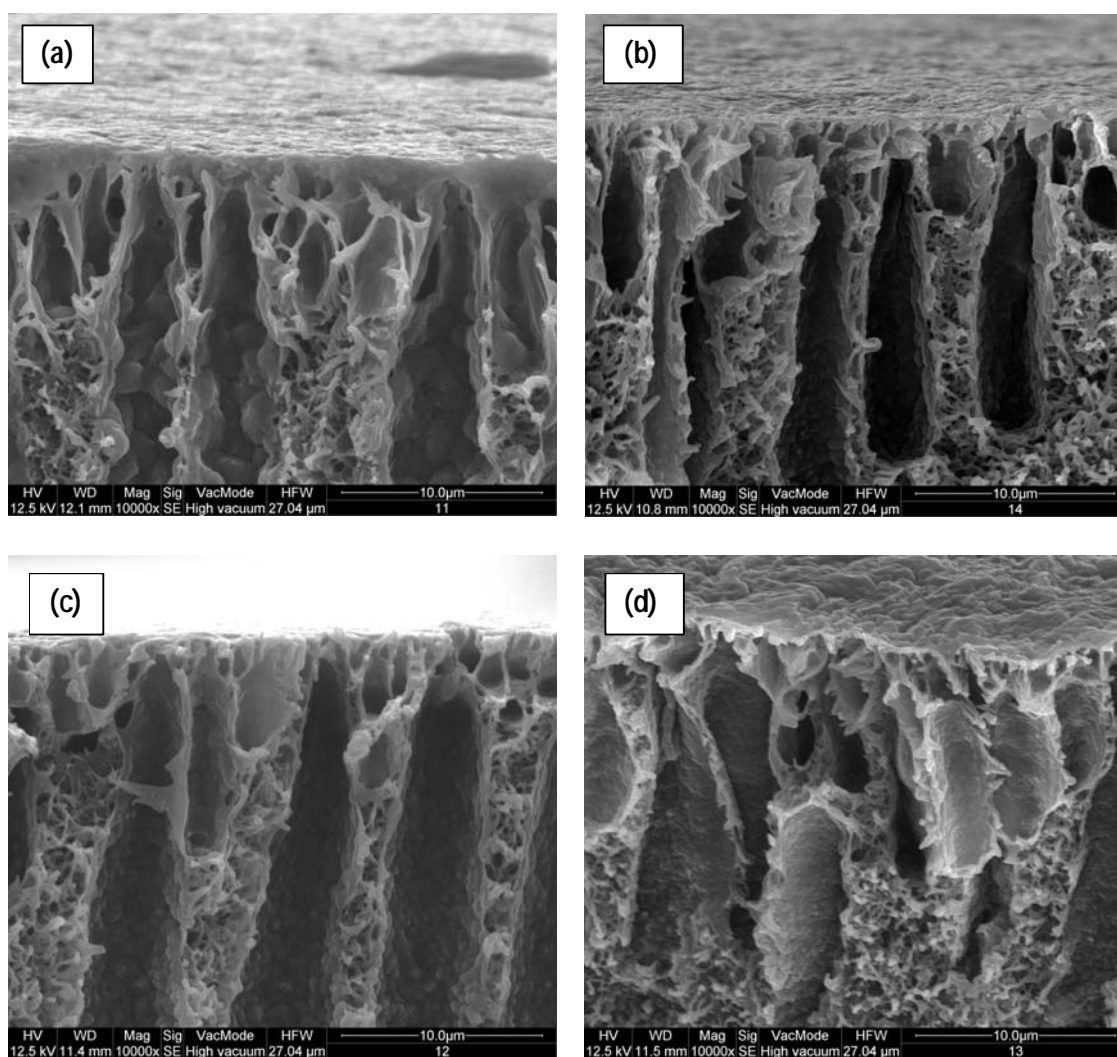


Figure 1: SEM micrographs of the investigated membranes. Cross-section of: a) unloaded PVDF; b) PVDF-15% Ag NPs; c) PVDF-20% Ag NPs; d) PVDF-25% Ag NPs.

The MD setup (schematized in Figure 2) consists of a dead-end cell with effective membrane area of 21.24 cm², with a quartz window mounted and sealed at the centre of the top lid. A high-pressure UV mercury lamp (Helios Ital Quartz srl) with peak wavelength of 366 nm and viewing angle of 90°, connected to GR.E. 500W portable power generator, was put above this quartz window and used to irradiate the membrane surface. Feed solution (0.5 M NaCl) was recirculated at 20 l/h by digital peristaltic pump Masterflex L/S (Cole Parmer, US). Temperature was monitored by Oakton Acorn® K-type thermocouple probe (Cole-Palmer, US) with response time of 15 sec and resolution of ±0.1°C. The system was operated under vacuum pressure of 20 mbar and initial feed temperature of 30°C (Vacuum Membrane Distillation, VMD).

Permeate conductivity was measured by YSI Model 3200 conductivity meter at 20°C (range: 0 to 49.99 μS/cm, accuracy: ±0.50% full scale, resolution: 0.01 μS/cm). Absence of Ag NPs in the permeate was confirmed by Dynamic Light Scattering (90Plus Particle Size Analyzer, Brookhaven Instruments Corporation, US), by sampling 50 μL of condensed VMD distillate in disposable plastic cells at room temperature.

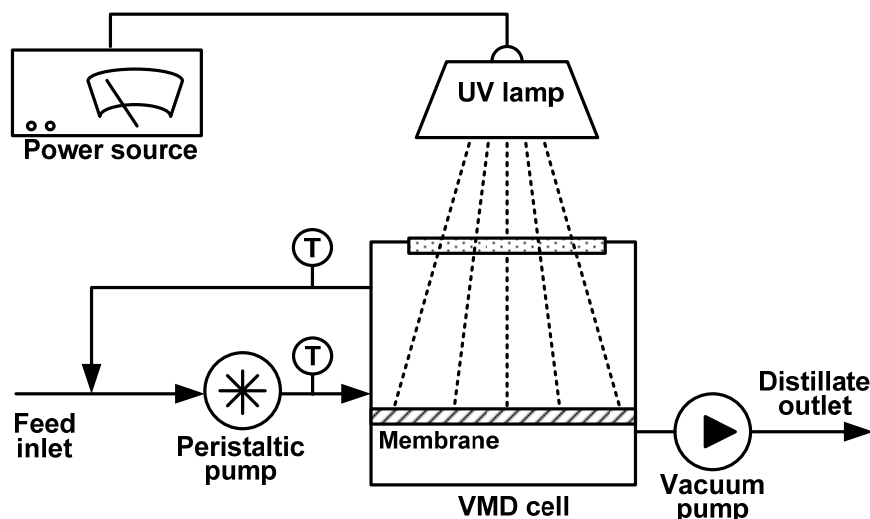


Figure 2: VMD setup.

3. Results and discussion

The impact of plasmonic heating effect on the performance of NPs-loaded PVDF membranes is illustrated in Figure 3a. The difference between outlet and inlet temperatures in the bulk of the feed stream increased with time, attaining a steady-state profile in about 30 minutes. For virgin PVDF membranes, UV irradiation raised the temperature difference by about 2.5°C. On the other hand, the outlet feed temperature increased at increasing NPs content in the polymeric matrix: at best, VMD cell equipped with PVDF-25% Ag NPs membrane resulted in a temperature increase of more than 4°C.

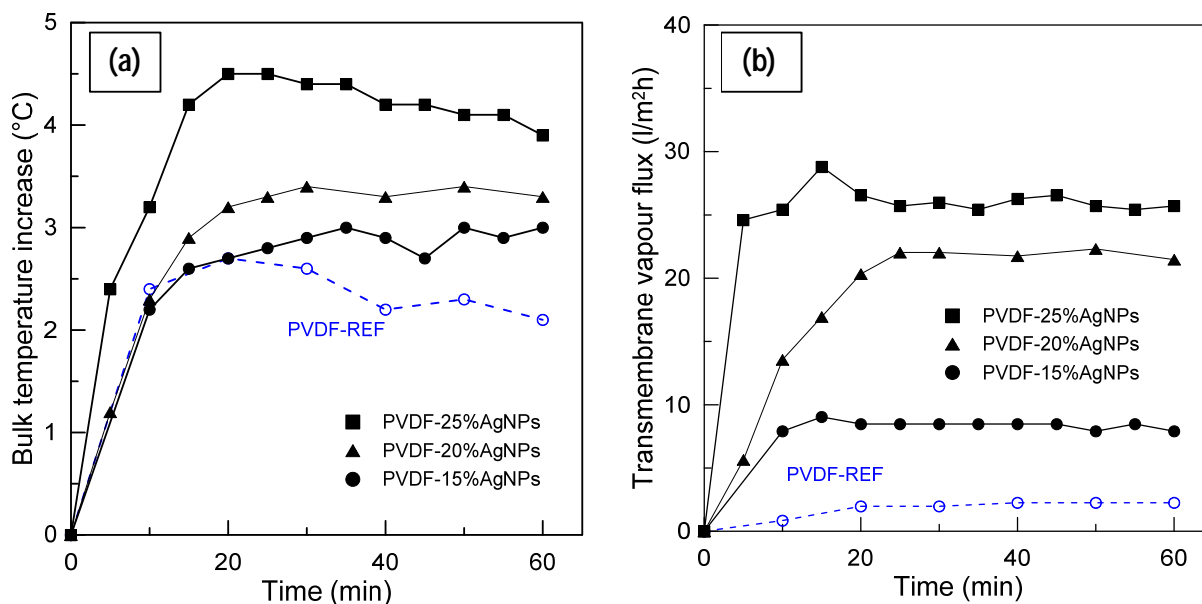


Figure 3: Time-variant performance of thermoplasmonic VMD system equipped with PVDF membranes at different Ag NPs content (feed: 0.5M NaCl solution): a) relative temperature increase in the bulk of the outlet feed stream with starting temperature of 30°C; b) transmembrane flux of water vapour.

Previous theoretical calculation showed that the amount of thermal energy produced by Ag NPs immobilized in the membrane is able to reverse the temperature polarization effect, leading to a interface feed temperature higher than that in the bulk (Politano *et al.*, 2017). Specifically, the plasmonics heat flux doubled the heat flux

associated to the latent evaporation heat through the membrane. As a result, for PVDF-25% Ag NPs membranes, the predicted steady-state increase of feed temperature at the interface was 24.2°C.

Time-variant transmembrane flux profiles over one hour of operation, for a 0.5M NaCl aqueous solution mimicking seawater salinity, are reported in Figure 3.b. The significantly lower vapour flux through unloaded PVDF membrane (~2.3 l/m²h) with respect to those measured for NPs-loaded membranes supports these findings. At best, the vapour flux through PVDF-25% Ag NPs at 60 min is 25.7 l/m²h, i.e. about 11-fold higher than the correspondent values for unloaded PVDF membranes.

The higher NPs content in the PVDF polymeric matrix, the higher flux enhancement is achieved. The increase of transmembrane flux is not linearly dependent on the Ag NPs concentration: flux increased by 170% when changing from PVDF-15% Ag NPs to PVDF-20% Ag NPs membrane, and by further 20% when adopting PVDF-25% Ag NPs membrane.

The analysis of structural characteristics of membranes reported in Table 1 clearly indicates that morphological modifications related to inclusion of NPs in the polymer matrix is not sufficient to justify such a significant enhancement of the transmembrane flux.

The analysis of the temperature profile across the boundary layer at feed side (as a result of polarization phenomenon) and of the effect of photothermal plasmonic excitation determined by metal NPs, provides a new insight on the potentialities of these innovative mixed matrix membranes.

A temperature polarization factor (TPF) is defined as:

$$\text{TPF}(\%) = \frac{T_{\text{feed,m}}}{T_{\text{feed,b}}} \times 100 \quad (1)$$

where $T_{\text{feed,m}}$ and $T_{\text{feed,b}}$ designate the feed temperature at the membrane interface and in the bulk, respectively. While $\text{TPF} < 100\%$ in conventional VMD, surprisingly, the thermal energy produced by plasmonic nanofillers reversed the polarization effect, leading to an interface feed temperature higher than in the bulk and, ultimately, to $\text{TPF} > 100\%$ (Figure 4). Energy balance based on experimental tests carried out with pure water confirmed that the photothermal heat flux overcame up to 1.7 times the latent heat flux associated to water evaporation through the microporous membrane.

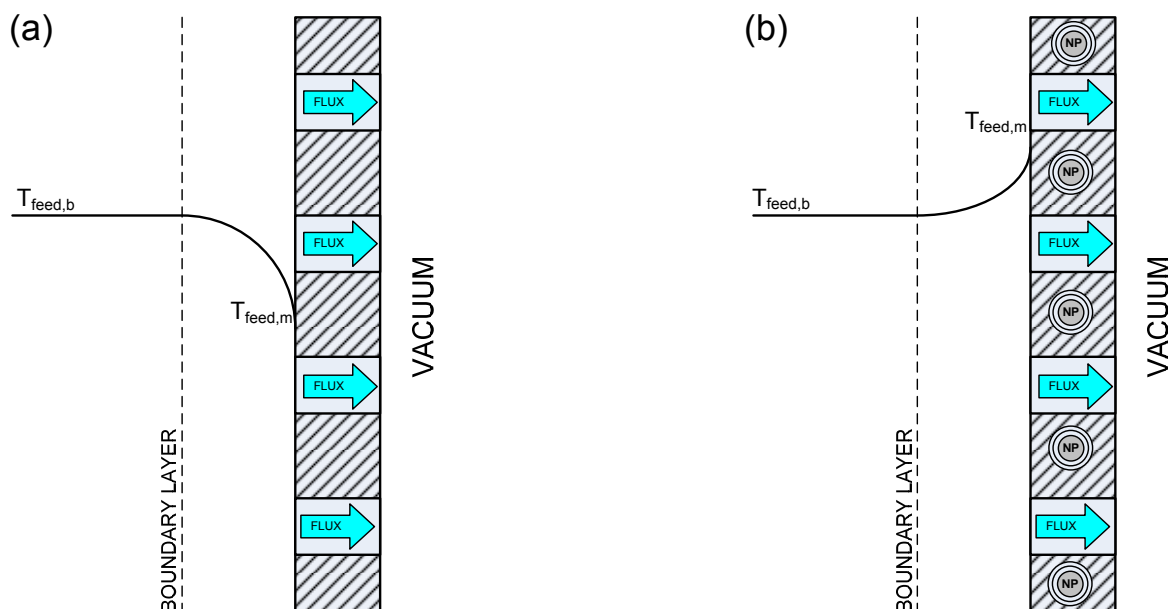


Figure 4: Thermal profile within the boundary layer at the feed side: (a) the temperature decreases from bulk to membrane surface for an unloaded membrane as a consequence of water evaporation (polarization phenomenon); (b) temperature polarization is reversed due to photothermal effects in Ag NPs-loaded membranes.

4. Conclusions

Herein, we have proven the effectiveness of thermoplasmonic MD technology. Thermal hotspots are activated at nanoscale by UV irradiation of PVDF membranes loaded with Ag nanoparticles. High thermal efficiency results from the removal of the temperature polarization. This experimental investigation provides evidence for a considerable enhancement of the transmembrane flux at the 25% w/w NPs concentration.

Although preliminary results show a considerable power consumption incompatible with industrial standards, significant energetic benefits are expected: i) by replacement of UV mercury lamp with light emitting diodes (LEDs) at customized wavelengths; ii) by using an aspirator (based on the Venturi effect) to generate low pressure for VMD unit; iii) by using solar energy to excite plasmon resonance in a wavelength range that covers the solar irradiation spectrum.

MD is not a competitor of Reverse Osmosis: the high compatibility of membrane operations, along with the well recognized ability of MD to efficiently operate at high salt concentration, can be synergistically exploited in integrated RO-MD processes. It has been proven that MD operated on RO retentate results in enhanced water quality and production capacity (overall recovery factor around 90%), thus improving the sustainability of desalination industry in the logic of Process Intensification (Drioli *et al.*, 2003).

References

- Al-Obaidani S., Curcio E., Macedonio F., Di Profio G., Al-Hinai H., Drioli E., 2008, Potential of membrane distillation in seawater desalination: thermal efficiency, sensitivity study and cost estimation, *J. Membrane Sci.* 323/1, 85-98
- Baffou G., Quidant R., 2013, Thermo-plasmonics: using metallic nanostructures as nano-sources of heat, *Laser Photon. Rev.* 7/2, 171-187
- Curcio E., Drioli E., 2005, Membrane distillation and related operations—a review, *Sep. Purif. Rev.* 34/1, 35-86
- Curcio E., Di Profio G., Drioli E., 2016, Microporous Hydrophobic Membranes for Crystallization of Biomolecules, *Chem. Eng. Trans.* 47, 421-426
- Di Profio G., Tucci S., Curcio E., Drioli E., 2007, Controlling polymorphism with membrane-based crystallizers: Application to form I and II of paracetamol, *Chem. Mater.* 19/10, 2386–2388
- Di Profio G., Curcio E., Drioli E., 2010, Supersaturation control and heterogeneous nucleation in membrane crystallizers: Facts and perspectives, *Ind. Eng. Chem. Res.* 49/23, 11878-11889
- Drioli E., Criscuoli A., Curcio E., 2003, Membrane contactors and catalytic membrane reactors in process intensification, *Chem. Eng. Technol.* 26/9, 975–981
- Hutter E., Fendler J. H., Roy D., 2001, Surface Plasmon Resonance Studies of Gold and Silver Nanoparticles Linked to Gold and Silver Substrates by 2-Aminoethanethiol and 1,6-Hexanedithiol, *J. Phys. Chem. B* 105, 11159-11168.
- Lattemann S., Höpner T., 2008, Environmental impact and impact assessment of seawater desalination, *Desalination* 220, 1–15
- Lee J., Govorov A.O., Dulka J., Kotov N.A., 2004, Bioconjugates of CdTe Nanowires and Au Nanoparticles: Plasmon–Exciton Interactions, Luminescence Enhancement, and Collective Effects, *Nano Lett.* 4/12, 2323–2330
- Majidi Salehi S., Di Profio G., Fontananova E., Nicoletta F.P., Curcio E., De Filipo G., 2016, Membrane distillation by novel hydrogel composite membranes, *J. Membrane Sci.* 504, 220-229
- Politano A., Argurio P., Di Profio G., Sanna V., Cupolillo A., Chakraborty S., Arafat H.A., Curcio E., 2017, Photothermal Membrane Distillation for Seawater Desalination, *Adv. Mat.* 29/2, 1603504
- Politano A., Cupolillo A., Di Profio G., Arafat H.A., Chiarello G., Curcio E., 2016, When plasmonics meets membrane technology, *J. Phys. Condens Matter* 28/36, 1-12
- Tufa R.A., Curcio E., Brauns E., van Baak W., Fontananova E., Di Profio G., 2015, Membrane Distillation and Reverse Electrodialysis for Near-Zero Liquid Discharge and low energy seawater desalination, *J. Membrane Sci.* 496, 325-333